Online Optimizing Control of Molecular Weight Properties in Batch Free-Radical Polymerization Reactors

Costas Kiparissides,*,† Panagiotis Seferlis,† George Mourikas,†,‡ and A. Julian Morris‡

Department of Chemical Engineering and Chemical Process Engineering Research Institute, Aristotle University of Thessaloniki, P.O. Box 472, 540 06 Thessaloniki, Greece, and Centre for Process Analytics, and Control Technology, School of Chemical Engineering and Advanced Materials, University of Newcastle, Newcastle upon Tyne NE1 7RU, U.K.

An online optimizing control scheme that ensures the satisfaction of the final polymer property specifications under the influence of time-varying model parameters and unknown initial conditions is developed for a batch polymerization reactor. The proposed control scheme combines a state/parameter estimator with an optimization step that calculates periodically the time optimal polymerization temperature based on the most recent information about the process. The state/parameter estimation step includes an extended Kalman filter for estimating the state variables and the time-varying termination rate constant of the model and a nonlinear optimization-based estimator for calculating the concentration of impurities at the start of the polymerization. The time optimal polymerization temperature that drives the process to the desired final polymer property specifications is determined using a dynamic programming technique based on the simultaneous discretization approach. A quadratic performance index is defined in terms of the squared differences between the achieved and desired values of final monomer conversion, number- and weight-average molecular weights, and the entire desired molecular weight distribution. The time optimal temperature policy is implemented, as a sequence of discrete set-point changes, by the regulatory control system of the reactor. The proposed control strategy manages to optimally satisfy the control objectives and keep the product quality indicators close to the desired levels in a least-squares sense by successfully alleviating the detrimental effects of process disturbances and model parameter variations.

Introduction

The operating objectives in batch polymerization processes must satisfy complex property requirements for the final polymer and simultaneously achieve the greatest economic potential during the batch operation. Meeting the specified targets during operation requires an increased effort in many different levels of the production procedure, such as the quality of the measurements, the accuracy of the model predictions, the performance of the control system, and the ability to determine and implement the optimal operating conditions that would ensure the satisfaction of certain economic and product quality criteria. Commonly employed polymer product quality indicators (e.g., mechanical strength, tear strength, rheological properties, and so forth) are directly or indirectly linked with the molecular structural properties of polymer chains (e.g., molecular weight distribution (MWD), copolymer composition distribution (CCD), chain sequence length distribution (CSD), and so forth), which are difficult (sometimes impossible) to measure online. Very often average polymer molecular weight properties (e.g., number- and weight-average molecular weights), which can be indirectly inferred from the online measurement of the solution viscosity or melt index of the polymer, are selected as the major controlled variables that need to be maintained within well-determined limits so that desired product quality criteria can be satisfied.

In theory, time optimal control policies that ensure the satisfaction of the polymer product property requirements and the operational constraints can be calculated offline and implemented as set-point changes of the regulatory control system. However, the operation of a polymerization reactor is heavily affected by disturbances resulting from a variety of process-related sources and an inherent model−process mismatch. Process interaction with upstream units or through recycle streams, modeling mismatch due to simplifying assumptions and unmodeled phenomena, variation of the model parameters due to changing operating conditions, and unmeasured process disturbances cause the plant to drift away from a predefined trajectory path. Thus, feedback of the error between the actual values of the controlled variables and the model predictions is required so that the control system can adjust the operating conditions (e.g., polymerization temperature, initiator concentration, and so forth) accordingly. The calculation of the optimal operating conditions depends on the adequacy of the process model, the values of the model parameters, and a knowledge of the unmeasured stochastic disturbances that affect the process.

The combined problem of state/parameter estimation and online optimization has been the subject of a number of research papers. Ponnuswamy et al.[1] pre-

* Corresponding author. Tel: +30 310 996 211. Fax: +30 310 996 198. E-mail: cypress@cperi.certh.gr.
† Aristotle University of Thessaloniki.
‡ University of Newcastle.

10.1021/ie0103409 CCC: $22.00
Published on Web 10/26/2002

sented an experimental and theoretical study on both open- and closed-loop optimal control of a batch polymerization reactor. A multivariable feedback controller was implemented to track the optimal state trajectories in the presence of process disturbances. Ruppen et al.[2,3] proposed an online parameter estimation−optimization scheme for a semibatch reactor, with the feed rate acting as the control variable. They showed clearly the benefits of the online approach against an approach where the operating profiles were defined a priori. Levien[4] discussed the optimization of batch reactors using discrete feed changes. Loeblein and Perkins[5] discussed the economic potential and the effect of the structural characteristics (e.g., estimated parameters, process measurements, controller set points) of the online optimization system in the presence of modeling and parametric uncertainty.

The work of Crowley and Choi[6,7] provides the most comprehensive study on the optimal control of the MWD in a batch free-radical polymerization experimental reactor. They proposed a control scheme incorporating a state estimator and an online optimizer that manages to follow the desired MWD by manipulating the temperature profile in the reactor. An extended Kalman filter (EKF) was used to retrieve the entire state vector based on process measurements (e.g., polymerization temperature, and conversion) and product quality variables (e.g., MWD). A model predictive control algorithm was implemented to track the suboptimal temperature profiles. However, they did not consider model parameter variations and process disturbances, which may affect severely the operation of the reactor. Furthermore, they used a piecewise constant-temperature profile of low resolution with long intervals of constant temperature as the optimal set-point sequence. Such a policy may fail to meet the product quality specifications under significant model parameter variations (e.g., termination rate constant variation due to the gel effect) and may be subject to aggressive set-point changes in temperature.

The present work deals with the online optimizing control of the number- and weight-average molecular weights as well as of the entire MWD of the polymer product in a free-radical batch polymerization reactor, operating under significant model parameter uncertainty. An online optimal polymerization temperature profile represented as a discrete sequence of temperature set-point changes is determined that can ensure the satisfaction of the product quality (e.g., average molecular weight properties) and process operating objectives (e.g., product yield and temperature constraints). An offline-calculated optimal polymerization temperature trajectory, based on time-invariant model parameters and neglecting the influence of process disturbances, will actually fail to meet the final product quality specifications and may lead to process constraint violations. On the other hand, the periodical updating of the optimal operating policy during a batch polymerization would significantly enhance the ability of the process to reach the target product quality specifications and guarantee the satisfaction of all process constraints. Hence, the deleterious effects of process disturbances and product quality drift caused by the model parameter variation can be alleviated. In the present study, an online estimator−optimization scheme is proposed for a free-radical batch polymerization reactor. The updating of the time optimal control policy is performed in two steps: a parameter estimation step that filters the process measurements to provide reliable estimates for the process states and time-varying model parameters and an optimization step that reevaluates periodically the time optimal polymerization temperature trajectory based on the most recent information about the process. The calculation of the time optimal control policy is obtained via dynamic programming techniques based on simultaneous discretization methods of the state and control variables.

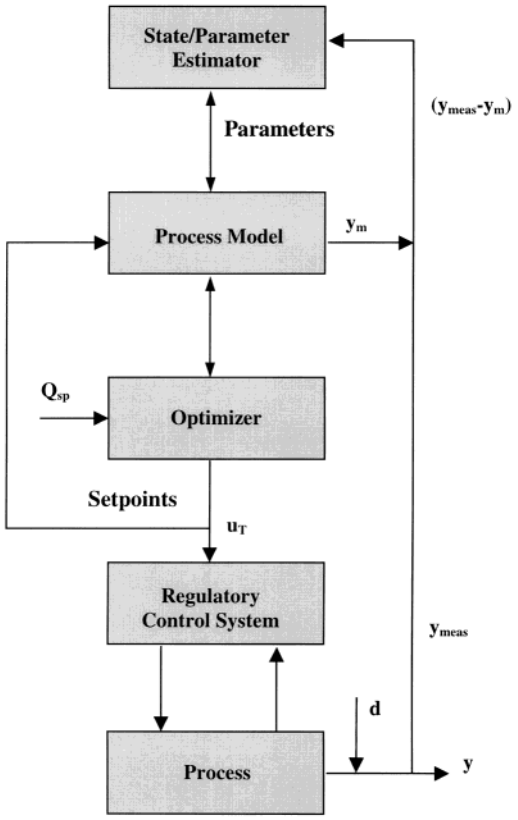

Figure 1. Schematic representation of the estimation−optimization control loop.

Problem Formulation

A schematic of the information flowsheet for the online optimizing controller is shown in Figure 1. The measured output variables vector, $\mathbf{y}_{meas}$, is compared to the model predictions vector, $\mathbf{y}_m$. The anticipated error incorporates the unmeasured process disturbances, **d**, and the measurement noise. The state/parameter estimation block uses the error term to retrieve the entire state vector of the system as well as estimates of the stochastic time-varying model parameters. It should be pointed out that observability requirements for states and parameters must be satisfied to accurately reconstruct the complete state/parameter vector. Subsequently, the updated values for the state variables and the model parameters are used by the optimizer block. A set of target values associated with the product quality characteristics, $\mathbf{Q}_{sp}$, and a performance index that specifies the overall process control objectives conclude the input stream to the optimization block. The optimizer calculates a series of optimal set-point changes for the control variables that would ensure the satisfaction of the overall process objectives in an optimal sense.

The optimal control trajectories are calculated for the remaining of the batch time based on the current estimates of the state variables and the model parameters. The online optimization task is very important, especially when significant changes in model parameters occur. The proposed nonlinear optimizer allows the evaluation of the optimal control actions over a wide range of operating conditions by taking into consideration the specified process constraints and bounds on the state and control variables. The execution of the optimization task is performed on a regular basis depending on the rate of change of the model parameters and the frequency of the process disturbances. The time optimal sequence of set-point changes, $\mathbf{u}_T$, is then passed to the regulatory controller that forces the process to follow the optimal trajectory as close as possible. Thus, the entire hierarchical control scheme includes a nonlinear optimizer, which utilizes the full nonlinear model to calculate an optimal sequence of set-point changes based on economic and product quality criteria, and a regulatory controller, which is responsible for the implementation of the optimal sequence of set-point changes. It should be pointed out here that the main aim is trajectory control without feedback correction for the dynamic process.

Nonlinear State and Parameter Estimation. In the present work, two types of estimators are employed, namely, an EKF for estimating the states and time-varying model parameters and an optimization-based estimator for calculating the initial values of the unknown state variables.

Let us assume that the dynamic behavior of the batch polymerization reactor is described by the following nonlinear system of differential equations:

$$\dot{\mathbf{x}} = \mathbf{f}(\mathbf{x},\mathbf{u},\mathbf{d},t) \tag{1}$$

$$\mathbf{y} = \mathbf{h}(\mathbf{x},\mathbf{u},\mathbf{d},t) \tag{2}$$

$$\mathbf{x} = \mathbf{x}_0(t=0) \tag{3}$$

f and **h** are vectors of continuous functions that represent the modeling relationships, **x**, **u**, and **y** are the corresponding state, input, and output vectors, **d** is the vector of unmeasured disturbances and unknown model parameters, and $\mathbf{x}_0$ is the vector of the initial conditions. The adaptation of the EKF algorithm for estimating the unknown model parameters and disturbances involves the addition of sensible stochastic states to the deterministic state vector. Thus, **x** is assumed to consist of two subsets, the deterministic part, $\mathbf{x}^d$, and the stochastic part, $\mathbf{x}^s$. The stochastic component, which includes the unknown model parameters and disturbances, may vary with time in some stochastic manner. Because the functional relationship $\mathbf{f}^s$ for the stochastic state variables is rarely known, the most common assumption, provided that $\mathbf{x}^s$ does not change considerably with time, is to be set equal to a zero vector. Thus, the dynamic behavior of the stochastic state variables is usually modeled as a random walk process. The inclusion of meaningful and consistent nonstationary stochastic state variables, $\mathbf{x}^s$, into the state/parameter estimator can eliminate the bias between the mathematical model and the actual process and provide good and unbiased state estimates.[8−10]

Given the current estimate of the state vector $\mathbf{x}(t_k/t_k)$ and after performance of a local linearization and discretization of the state model around the current estimate $\mathbf{x}(t_{k+1}/t_k)$, the state vector at t_{k+1} is obtained:

$$\mathbf{x}_{k+1} = \mathbf{F}_k\mathbf{x}_k + \mathbf{w}_k \tag{4}$$

$$\mathbf{y}_k = \mathbf{H}_k\mathbf{x}_k + \mathbf{v}_k \tag{5}$$

where

$$\mathbf{x}_k = \begin{bmatrix}\mathbf{x}_k^d\\ \mathbf{x}_k^s\end{bmatrix} \qquad \mathbf{F}_k = \begin{bmatrix}\mathbf{F}_k^d & \mathbf{F}_k^s\\ 0 & I\end{bmatrix} \qquad \mathbf{w}_k = \begin{bmatrix}\mathbf{w}_k^d\\ \mathbf{w}_k^s\end{bmatrix}$$

$\mathbf{F}_k$ and $\mathbf{H}_k$ are the Jacobian matrices of $\mathbf{f}(\mathbf{x},\mathbf{u},t)$ and $\mathbf{h}(\mathbf{x},\mathbf{u},t)$ with respect to **x**. The stochastic components $\mathbf{w}_k$ and $\mathbf{v}_k$, corresponding to the process and measurement noise, respectively, are assumed to be zero-mean white Gaussian frequencies with covariance matrices **Q** and **R**, respectively. When a new observation becomes available, the states are updated according to the following equation:

$$\mathbf{x}(t_{k+1}/t_{k+1}) = \mathbf{x}(t_{k+1}/t_k) + \mathbf{K}(t_k)\{\mathbf{y}(t_{k+1}) - \mathbf{h}(\mathbf{x}(t_{k+1}/t_k),\mathbf{u}(t_{k+1}),t_{k+1})\} \tag{6}$$

$\mathbf{K}(t_k)$ is the Kalman gain at time t_k computed recursively from the resulting Riccati equations.[9,10]

The problem of identifying the unknown initial stochastic states (e.g., initial concentration of impurities) is of great importance for the robust online implementation of an EKF to a batch polymerization reactor. Standard EKFs are purely recursive estimators that never go back in time to reprocess past data and correct errors that took place in earlier stages of the reaction. Therefore, in the case of unknown initial states, an optimization-based batchwise estimator[11] is employed to calculate the unknown initial state vector $\mathbf{x}(t_0/t_k)$ each time new measurements, $\mathbf{y}(t_k)$, become available. The optimization-based estimator uses the full nonlinear process model (eqs 1−3) without any assumptions on the type of process and measurement errors to calculate the unknown initial state variables by minimizing an objective function over a past time horizon. The horizon moves forward in time as new measurements become available and, thus, the estimator is suitable for online implementation. The unknown initial conditions to be estimated are included in the state vector as additional stochastic states. The estimator computes in its general form the unknown initial states, $\mathbf{x}(t_0/t_k)$, and model corrections, $\mathbf{w}(t_j/t_k)$, by minimizing the following quadratic objective function:

$$J_k = [\mathbf{x}(t_0/t_k) - \mathbf{x}(t_0)]^T \mathbf{P}_{0,BE}^{-1} [\mathbf{x}(t_0/t_k) - \mathbf{x}(t_0)]^T + \sum_{j=1}^{k-1} \mathbf{w}^T(t_j/t_k)\, \mathbf{Q}_{BE}^{-1} \mathbf{w}(t_j/t_k) + \sum_{j=1}^{k} \mathbf{v}^T(t_j/t_k)\, \mathbf{R}_{BE}^{-1} \mathbf{v}(t_j/t_k) \tag{7}$$

subject to the following constraints:

$$\mathbf{w}(t_j/t_k) = \mathbf{x}(t_{j+1}/t_k) - \mathbf{f}(\mathbf{x}(t_j/t_k),\mathbf{u}(t_j),\mathbf{d})$$

$$\mathbf{v}(t_j/t_k) = \mathbf{y}_{meas}(t_j) - \mathbf{h}(\mathbf{x}(t_j/t_k),\mathbf{u}(t_j),\mathbf{d})$$

$$\mathbf{c}_j^{min} \le \mathbf{C}\mathbf{x}(t_j/t_k) \le \mathbf{c}_j^{max}$$

$$\mathbf{w}_j^{min} \le \mathbf{w}(t_j/t_k) \le \mathbf{w}_j^{max} \qquad \text{for } j = 1, \ldots, k \tag{8}$$

where $\mathbf{w}(t_j/t_k)$ and $\mathbf{v}(t_j/t_k)$ are the respective process and measurement disturbance vectors, estimated at time t_j

based on the available information up to the kth sampling interval. The weighting matrices $\mathbf{Q}_{BE}$ and $\mathbf{R}_{BE}$ specify the relative contribution of the two terms to the quadratic objective function and are actually the tuning parameters of the least-squares estimator. The choice of the weighting matrices is based upon a compromise between the minimization of the estimated process and measurement errors. A simple and often successful initial choice is to use the inverse of the nonsingular covariance matrices for process and measurement disturbances, respectively. $\mathbf{P}_{0,BE}$ is an additional tuning matrix and accounts for the degree of uncertainty in the initial values of the state variables. The use of state and process disturbance bounds (e.g., constraint matrix $\mathbf{C}$ and bounds $\mathbf{c}^{min}$ and $\mathbf{c}^{max}$) excludes solution values with no physical meaning and restricts the moves of the optimization variables within certain limits.

Calculation of the Time Optimal Control Trajectories. The major goal of the optimization task is to determine a sequence of set-point changes for the control variables that would satisfy a certain performance criterion. The process control variables are selected based on their impact on the product quality and process ability for real-time implementation. For example, in the case of methyl methacrylate (MMA) free-radical polymerization, the reactor temperature plays the most important role in controlling the final polymer properties (e.g., average molecular weights, M_n and M_w). Other examples of optimization variables could be the initiator concentration in the reactor or the initiator feed rate.

The performance index usually depends on the final state of the system and the dynamic characteristics of the batch polymerization. In general, the dynamic optimization problem can be stated as

$$\min_{\mathbf{u}_T,t_f} J = G(\mathbf{x}(t_f),\mathbf{y}(t_f),\mathbf{d},t_f) + \int_{t_0}^{t_f} L(\mathbf{x}(t),\mathbf{y}(t),\mathbf{u}_T(t),\mathbf{d},t)\,dt$$

$$\text{s.t.} \quad \dot{\mathbf{x}} = \mathbf{f}(\mathbf{x},\mathbf{u}_T,\mathbf{d},t)$$

$$\mathbf{y} = \mathbf{h}(\mathbf{x},\mathbf{u}_T,\mathbf{d},t)$$

$$0 \le \mathbf{g}(\mathbf{x},\mathbf{u}_T,\mathbf{d},t) \qquad \text{(P1)}$$

where t_0 and t_f denote the initial and final batch times. G and L are scalar functionals. The functions $\mathbf{f}$, $\mathbf{h}$, and $\mathbf{g}$ comprise the modeling equality and inequality constraints that must be satisfied at all times. The vector $\mathbf{u}_T(t)$ denotes a time optimal control trajectory (e.g., temperature profile) that causes the batch system to follow an admissible trajectory and minimizes the performance index J in (P1). Vector $\mathbf{d}$ denotes the values of the model parameters and process disturbances. The total duration of the batch, t_f, may be treated as an additional decision variable or may be considered constant. The dynamic behavior of the state variables is governed by differential equations, while constitutive expressions and operating constraints are described by algebraic equations.

The optimization problem (P1), which generally involves large sets of differential and algebraic equations (DAEs), can be solved either using Pontryagin's maximum principle[12,13] or the more powerful and efficient, especially for large-scale problems, discretization methods. A great number of publications have appeared in the open literature dealing with the solution of dynamic optimization problems using discretization methods. The various discretization algorithms can be classified into two groups: (i) the simultaneous solution method,[14−16] where both the state and the control vectors are discretized in time, leading to the transformation of the DAE system into a set of purely algebraic equations, and (ii) the sequential solution method,[17] where only the control vector is parametrized in time. In the simultaneous approach, the resulting system of algebraic equations is solved using any conventional large-scale nonlinear programming method. On the other hand, in the sequential approach the resulting DAE system is solved in an independent step with the help of a DAE integrator. In this case, the integrator conveys sensitivity information to the optimizer and receives in response from the optimizer the calculated discrete optimal control values.

The simultaneous approach provides a unified framework for the simulation, optimization, and control of complex processes. It is very powerful in handling explicitly constraints but suffers from a large inflation of the size of the resulting set of algebraic equations, especially when the DAE system is stiff. On the other side, the sequential approach utilizes very efficient DAE integrators with reliable error control strategies and solves optimization problems of relatively small size. However, it requires the integration of the DAE system at every iteration, thus handling the process constraints indirectly.

In the present study, the method of orthogonal collocation on finite elements (OCFE) was employed to discretize the original DAE system into a set of algebraic equations. According to the OCFE formulation, the entire time domain was divided into a number of N_e subdomains called finite elements. The variation of state and control variables within each finite element was approximated by Lagrange polynomials of known order, expressed in terms of position in time and the values of the corresponding state and control variables at specified points (e.g., collocation points). The main assumption in the OCFE formulation is that the modeling equations are satisfied exactly only at the distinct collocation points within each time subdomain. The collocation points were selected as the roots of the Legendre orthogonal polynomials (Jacobi polynomials may also be an alternative choice). Continuity of the state profiles was ensured through the boundary conditions at the element breakpoints [$\tau_0 = t_0, \tau_1, \tau_2, ..., \tau_{N_e} = t_f$]. Very often the control variable is treated as a piecewise constant while discontinuity always occurs at an element breakpoint.

Based on the above discretization approach (OCFE), the optimization problem (P1) takes the following form:

$$\min_{\tilde{\mathbf{u}}_{T,j}(t_i),t_f} J = \tilde{G}(\tilde{\mathbf{x}}_{N_e}(t_i),\tilde{y}_{N_e}(t_i),\mathbf{d},t_i) + \sum_{k=1}^{N_e}\int_{\tau_{k-1}}^{\tau_k} \tilde{L}(\tilde{\mathbf{x}}_k(t_i),\tilde{\mathbf{y}}_k(t_i),\tilde{\mathbf{u}}_{T,k}(t_i),\mathbf{d},t_i)\,dt$$

$$\text{s.t.} \quad \dot{\tilde{\mathbf{x}}}_j = \mathbf{f}(\tilde{\mathbf{x}}_j(t_i),\tilde{\mathbf{u}}_{T,j}(t_i),\mathbf{d},t_i)$$

$$\tilde{\mathbf{y}}_j = \mathbf{h}(\tilde{\mathbf{x}}_j(t_i),\tilde{\mathbf{u}}_{T,j}(t_i),\mathbf{d},t_i)$$

$$0 \le \mathbf{g}(\tilde{\mathbf{x}}_j(t_i),\tilde{\mathbf{u}}_{T,j}(t_i),\mathbf{d},t_i)$$

$$j = 1, ..., N_e; \quad i = 1, ..., n_j \qquad \text{(P2)}$$

The tilde denotes approximation variables.

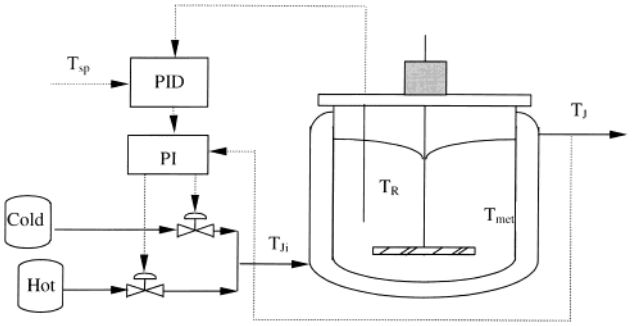

Figure 2. Schematic representation of the simulated pilot-plant batch free-radical polymerization reactor.

The OCFE formulation requires a sufficient number of collocation points for an accurate representation of the actual time variation of the state variables. Strategies for adaptive placement of element breakpoints[18] can handle situations with steep state profiles by increasing the density of the collocation points in the region where the states change rapidly. This can be achieved by proper placement of small in size finite elements near the steep fronts. Larger elements with the same number of collocation points can provide an accurate approximation in regions where the states have relatively flat profiles. However, because the variation of the state variables is not known a priori, the element breakpoints can be treated as additional degrees of freedom that are allowed to move during the optimization problem, resulting in adaptive OCFE schemes.[15,19] Systems of stiff differential equations are characteristic examples, where adaptive OCFE schemes should be applied.[20]

Optimizing Control of a Batch Polymerization Reactor

The estimation−optimization scheme outlined in Figure 1 was applied to a simulated model of a free-radical MMA batch polymerization reactor (see appendix A). The mathematical model closely described the dynamic behavior of the experimental pilot-scale system (see Figure 2) operated at our laboratory. Heating and cooling of the reaction mixture was achieved by controlling the flows of two water streams (e.g., a hot and a cold one) through the reactor jacket. The polymerization temperature was controlled by a cascade control system consisting of a primary proportional−integral−derivative (PID) and two secondary PI controllers. The polymerization was highly exothermic and exhibited a strong acceleration in the polymerization rate due to the gel effect (e.g., the termination rate constant decreased with conversion).

The state variables included the reactor volume, the monomer conversion, the initiator concentration, the three leading moments of the number chain-length distribution (NCLD) of the "live" polymer chains, the three leading moments of the NCLD of the "dead" polymer chains, and the reactor and jacket temperatures (see eqs A1−A11 in appendix A). Available online measurements included the reactor and jacket temperatures and the monomer conversion. The measurements did not provide all of the required information to reconstruct the entire state vector, thus leaving the moments of the "live" NCLD and the zeroth and second moments of the "dead" NCLD unobservable. To make these states observable, molecular weight measurements are required, which, however, are quite difficult to obtain online.

The polymerization temperature was selected as the control variable because of its profound effect on the reaction kinetics and, consequently, on the final molecular weight properties and monomer conversion. Furthermore, an optimal temperature trajectory could be easily implemented by the regulatory cascade control system of the reactor (Figure 2).

Computational Aspects. An OCFE technique was employed to discretize the set of model differential equations (A1)−(A11). Accordingly, the time domain was divided into a number of equispaced elements, N_e, with each element representing a fraction (t_f/N_e) of the total batch polymerization time, t_f. The number of finite elements dictated the accuracy of the approximation of the time optimal control trajectory. Within each element, three collocation points, defined by the roots of a third-order Legendre polynomial, were chosen. The state variables were approximated within each element using a fourth-order Lagrange polynomial (three interior collocation points plus the initial point for each element). Continuity for the state variables was assured at the element breakpoints with the addition of the proper boundary conditions.

To calculate the weight chain-length distribution of PMMA, an OCFE method was employed (see appendix B). The major points of the OCFE formulation can be found in a recent publication by Seferlis et al.[21] The OCFE formulation preserved the structure of the material balances for the "live" and "dead" polymer chains but required a much smaller number of modeling equations that facilitated significantly the solution procedure and made it attractive for online control and optimization applications. A key characteristic of the OCFE formulation was the treatment of the discrete polymer chain-length domain, S_f, as a continuous one. Hence, the variables that were associated with the polymer chain length, such as the concentrations of the "live" and "dead" polymer chains, were treated as continuous variables. The total chain-length domain was selected to be equal to 114 400 monomer units and was divided into eight finite elements of the following sizes: 200, 200, 1000, 1000, 2000, 10 000, 50 000, and 50 000. Two collocation points were selected within each element.

The online optimization block calculated the optimal sequence of temperature set-point changes for the batch reactor that minimized the following performance index:

$$J = w_1\frac{t_f}{t_d} + w_2\left(\frac{X_f}{X_d} - 1.0\right)^2 + w_3\left(\frac{M_{n,f}}{M_{n,d}} - 1.0\right)^2 + w_4\left(\frac{M_{w,f}}{M_{w,d}} - 1.0\right)^2 + w_5\sum_{i=1}^{nc}\left(\frac{WCLD_{i,f}}{WCLD_{i,d}} - 1.0\right)^2 \quad (9)$$

where X_f, $M_{n,f}$, $M_{w,f}$, and $WCLD_{i,f}$ are the values of monomer conversion and number- and weight-average molecular weights and the discrete values of the weight chain-length distribution (WCLD) at the final time t_f, respectively. X_d, $M_{n,d}$, $M_{w,d}$, and $WCLD_{i,d}$ are the corresponding desired values of the polymer quality variables. Deviations from the target values of the polymer quality variables would have a substantial impact on the economics of the process (e.g., the product value may drop or the entire batch content may have to be discarded). On the other hand, the conversion target, X_d, depicts the intention to maximize reactor productiv-

ity. The weighting factors, w_1-w_5 in eq 9, specify the relative importance of the corresponding competing terms.

A major decision for the entire optimization problem is the type of approximation used for the polymerization temperature trajectory within each finite element. It should be pointed out that, by varying the total number of decision variables (e.g., number of discrete temperature values), different optimal solutions and, thus, final product properties can be obtained. Obviously, a continuous-time optimal temperature trajectory would result in a smaller value of the performance index (eq 9) than a piecewise constant trajectory. However, such a choice suffers from practical implementation problems. Furthermore, the selection of the number of discrete temperature values is also related with the dynamic characteristics of the regulatory control system and its ability to trace the calculated optimal profile. In the present study, the time optimal temperature trajectory was approximated by a piecewise constant profile within each finite element, N_e. The final nonlinear programming problem consisted of 80 temporal elements and involved 7383 variables, 7320 constraints, and 22 initial conditions with 41 degrees of freedom.

The optimization problem was solved with the aid of a MINOS 5.3 nonlinear optimizer,[22] which uses an augmented Lagrangian reduced-gradient type of algorithm. Unless a global optimization type of algorithm is used for the solution of (P2), only a local Karush−Kuhn−Tucker optimal point can be calculated for the general nonconvex set of constraints. As a result, a suboptimal sequence of set-point changes could be obtained by the present solution algorithm. The performance of the proposed optimal control scheme was examined under two different mismatch scenarios: (i) process−model mismatch caused by variation of the termination rate constant, k_t, due to the gel effect and (ii) process−model mismatch caused by an erroneous initial initiator concentration due to the presence of an unknown amount of reactive impurities.

Time-Varying Kinetic Parameters. In free-radical polymerization, the termination rate constant can vary with monomer conversion due to the gel effect. In general, the termination rate constant can be expressed in terms of an intrinsic chemical rate constant, k_{t0}, and a diffusion-controlled function, g_t[23,24] (see eq A14), accounting for the observed decrease of k_t with monomer conversion. However, the gel-effect function, g_t, includes a number of parameters which are often unknown. Thus, the contribution of g_t to the termination rate constant involves a significant source of uncertainty. In the present study, a correction term, $g_{t,corr}$, was employed to account for the imprecise knowledge of g_t. As a result k_t was expressed as a product of three terms:

$$k_t = k_{t0} g_t g_{t,corr} \tag{10}$$

An EKF was employed to provide estimates for the process state variables and the time-varying parameter, $g_{t,corr}$. It was assumed that the unknown parameter, $g_{t,corr}$, followed a random walk model:

$$g^s_{t,corr} = w^s \tag{11}$$

where w^s is a zero-mean white Gaussian noise.

The time optimal polymerization temperature that minimized the objective function (eq 9) was calculated for two different polymer grades (e.g., A and B). The polymer quality specifications for grades A and B were ($M_{n,d} = 4.0 \times 10^5$ kg/kmol, $M_{w,d} = 2.0 \times 10^6$ kg/kmol, $x_d = 0.85$) and ($M_{n,d} = 5.0 \times 10^5$ kg/kmol, $M_{w,d} = 1.5 \times 10^6$ kg/kmol, $x_d = 0.85$), respectively. A target WCLD was also specified for both grades. All other information regarding kinetic rate constants, physical properties, are process operating conditions is given in Tables 1 and 2. Table 3 provides the values of the tuning parameters for the discrete PI and PID controllers as well as the tuning parameters for the EKF estimator. The discrete time interval of the primary and secondary temperature controllers was set equal to 15 s. The state variables and the time-varying model parameter, $g^s_{t,corr}$, were estimated every 2 min, while a new optimal temperature trajectory was evaluated every 20 min (unless stated otherwise) using the most recent value of the termination rate constant.

In the simulated process−model mismatch case with respect to the termination rate constant, the value of the $g_{t,corr}$ term in eq 10 was assumed to increase or decrease linearly with time according to the following law: $g_{t,corr} = 1 \pm ct$. Notice that an increase in the value of $g_{t,corr}$ indicated a positive disturbance scenario. On the other hand, a decrease in the value of $g_{t,corr}$ represented a negative disturbance scenario. The positive disturbance scenario (e.g., $g_{t,corr} = 1 + ct$) forced the termination rate constant to follow a steeper decrease than in the nominal case ($g_{t,corr} = 1$), while the opposite occurred during a negative disturbance scenario (e.g., $g_{t,corr} = 1 - ct$).

Figure 3 depicts the time optimal temperature profiles at different time instances, calculated through successive state/parameter estimation and optimization steps, for grade A (high polydispersity index) and a positive disturbance scenario (e.g., $g_{t,corr}$ increases with time).

Table 1. Kinetic Rate Constants[23]

$f_i = 0.58$
$k_d = 6.32 \times 10^{16} \exp(-30600/RT)$, 1/min
$k_{po} = 2.95 \times 10^7 \exp(-4350/RT)$, m^3/(kmol min)
$k_{to} = 5.88 \times 10^9 \exp(-701/RT)$, m^3/(kmol min)
$k_f/k_p = 9.48 \times 10^3 \exp(-13880/RT)$
$k_{tc}/k_{td} = 3.956 \times 10^{-4} \exp(4090/RT)$
$k_{td} = k_t - k_{tc}$, m^3/(kmol min)
$A = (0.168-8.21) \times 10^{-6}(T - 387.2)^2$; $B = 0.03$
$\theta_t = 1.1353 \times 10^{-22} \exp(17420/T)/I_0$
$\theta_p = 5.4814 \times 10^{-16} \exp(13982/T)$

Table 2. Physical Properties and Reactor Operating Conditions

Physical Properties	
$\rho_m = 1302 - 1225T$ kg/m^3	$C_{\rho_p} = 1.674$ kJ/(kg K)
$\rho_p = 1200$ kg/m^3	$C_{\rho_w} = 4.297$ kJ/(kg K)
$\rho_w = 982$ kg/ m^3	$\Delta H_R = 53.922$ kJ/mol
$C_{\rho_m} = 1.674$ kJ/(kg K)	MW = 100.15 kg/kmol
Initial Concentrations	
$I_0 = 4 \times 10^{-3}$ kg	$M_0 = 1.1$ kg
Reactor Parameters	
$V_o = 1.2 \times 10^{-3}$ m^3	$V_j = 3.795 \times 10^{-3}$ m^3
UA = 25.0 kJ/(K min)	

Table 3. Controller Settings and EKF Tuning Parameters

Primary Loop

$K_c = 1.5$, $\tau_I = 2.0$, $\tau_d = 0.2$

Secondary Loop

$K_c = 0.0008$, $\tau_I = 10.5$

EKF Tuning Parameters

$\mathbf{P}_0 = [10^{-6}, 10^{-6}, 10^{-6}, 10^{-6}, 10^{-6}, 10^{-6}, 10^{-6}, 10^{-6}, 10^{-6}, 10^{-6}, 10^{-6}, 10^{-2}]$
$\mathbf{Q} = [10^{-8}, 10^{-6}, 10^{-8}, 10^{-12}, 10^{-12}, 10^{-12}, 10^{-12}, 10^{-12}, 10^{-12}, 10^{-6}, 10^{-6}, 5.0]$
$\mathbf{R} = [10^{-3}, 10, 10]$

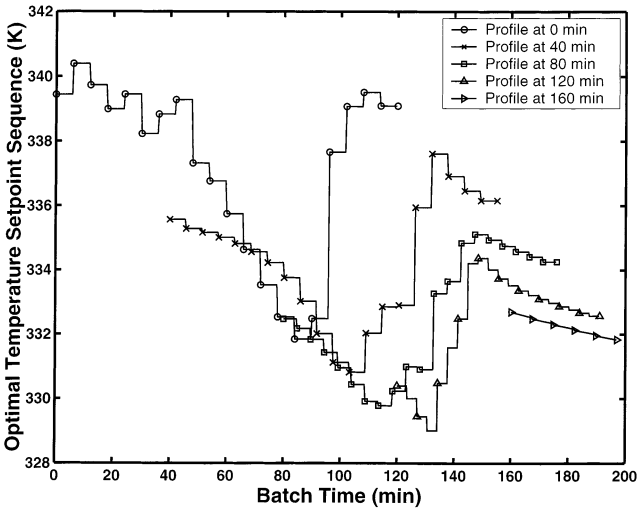

Figure 3. Updated time optimal temperature trajectories for grade A and a positive disturbance scenario in k_t ($g_{t,corr} = 1 + 8.0 \times 10^{-3}t$).

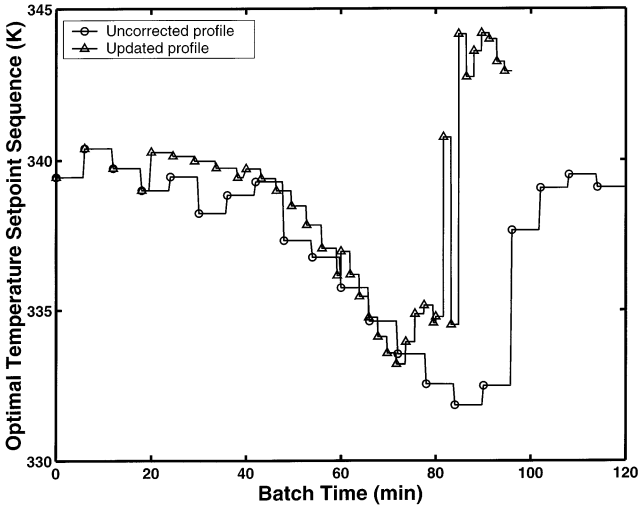

Figure 4. Updated time optimal temperature trajectories for grade A and a negative disturbance scenario in k_t ($g_{t,corr} = 1 - 4.0 \times 10^{-3}t$).

Notice that the updated time optimal temperature profiles differ from the polymerization temperature profile calculated at the beginning of the batch in both shape and duration due to the process−model mismatch caused by the variation in the termination rate constant. It is also important to mention that, because of the appearance of the gel effect, the optimal temperature trajectory passes through a minimum value and increases right after it to maintain the molecular weight averages (M_n and M_w) and the WCLD near their respective desired values. It should be pointed out that the positive disturbance scenario resulted in an increase of the total polymerization time from $t_f = 120$ min (e.g., nominal case) to $t_f = 197$ min.

Figure 4 shows the time optimal temperature profiles at different time instances, calculated through successive state/parameter estimation and optimization steps (thin lines) for grade A and a negative disturbance scenario. Notice that the negative disturbance scenario results in a total batch time of 97 min, shorter by 23 min of the nominal batch time of 120 min. The effect of the weighting factor w_1 in the performance index (eq 9) on the calculated time optimal profile is shown in Figure 5 for two values of w_1, namely, $w_1 = 1.0$ and 10.0. It

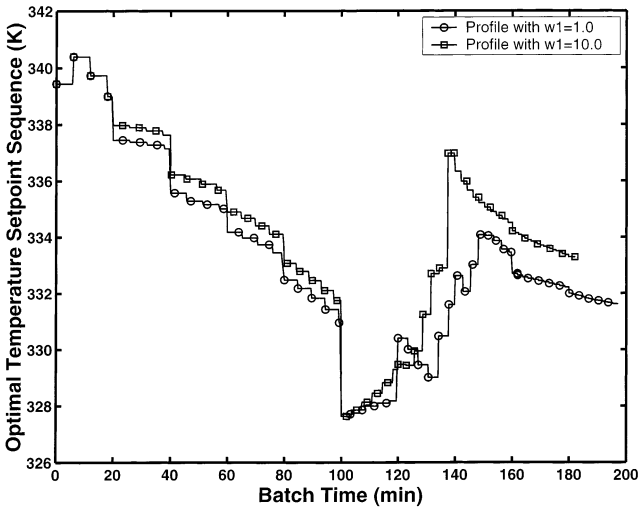

Figure 5. Updated time optimal temperature trajectories for grade A and a positive disturbance scenario for two values of the weighting coefficient, w_1, in the objective function (eq 11).

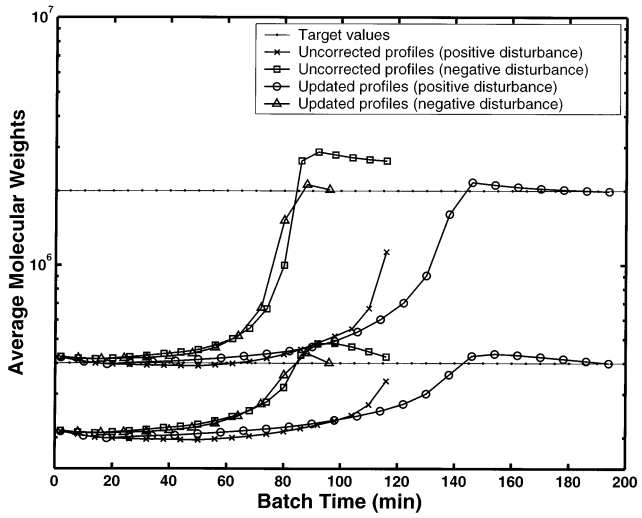

Figure 6. Uncorrected and updated number- and weight-average molecular weight profiles for grade A.

can be seen that a larger w_1 reduces the total batch time from 197 min for $w_1 = 1.0$ to 182 min for $w_1 = 10.0$ but results in greater deviations of the quality variables from their respective desired final values.

In Figure 6 the average molecular weights corresponding to the uncorrected and updated temperature profiles are plotted with respect to the batch time. Notice that the number- and weight-average molecular weights exhibit a sharp increase upon the onset of the gel effect caused by the decrease in the termination rate constant. In both cases (e.g., positive and negative disturbance scenarios), the online calculated optimal temperature policies force the system to the desired target values of M_n and M_w despite the presence of unknown disturbances in k_t. Figure 7 shows the time evolution of the WCLD of PMMA. It can be seen that the final WCLD coincides with the desired target WCLD. The results of Figures 6 and 7 indicate that the updated temperature trajectories result in a definite improvement of the final product properties and successfully compensate for the effect of the time-varying termination rate constant, k_t.

In Figure 8 the time optimal temperature trajectories are plotted for grade B and a positive disturbance

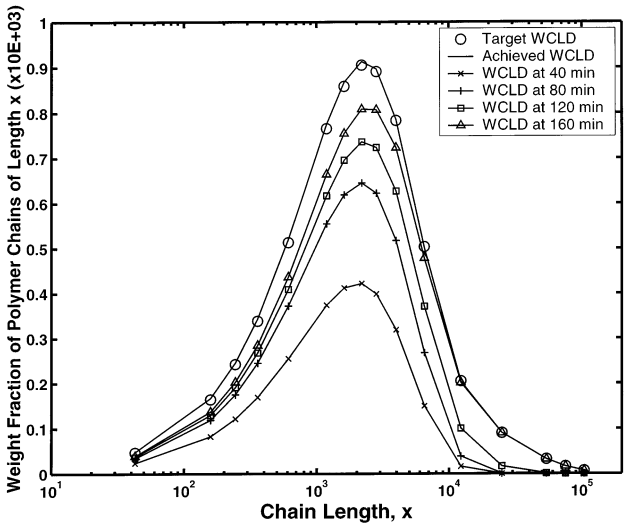

Figure 7. Time evolution of WCLD for grade A.

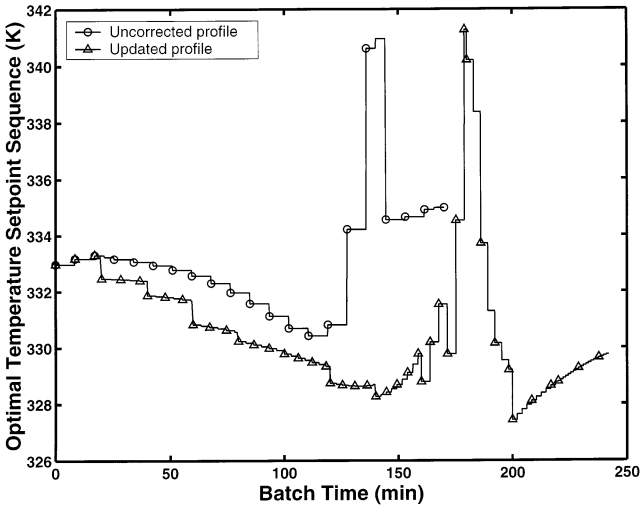

Figure 8. Updated time optimal temperature set-point sequences for grade B and a positive disturbance scenario in k_t ($g_{t,corr} = 1 + 4.0 \times 10^{-3}t$).

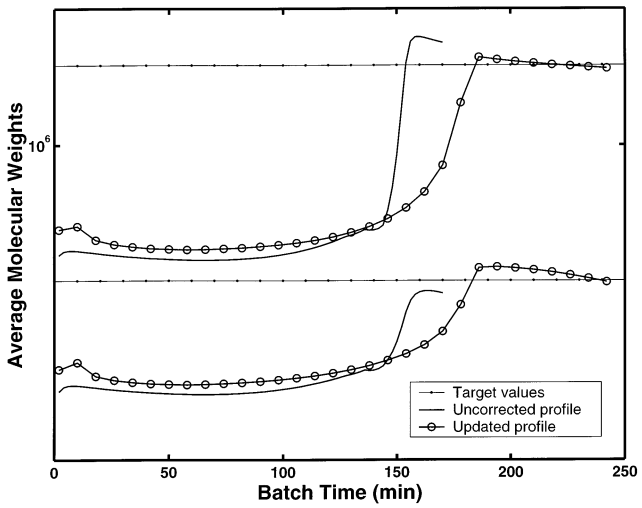

Figure 9. Uncorrected and updated number- and weight-average molecular weight profiles for grade B and a positive disturbance scenario.

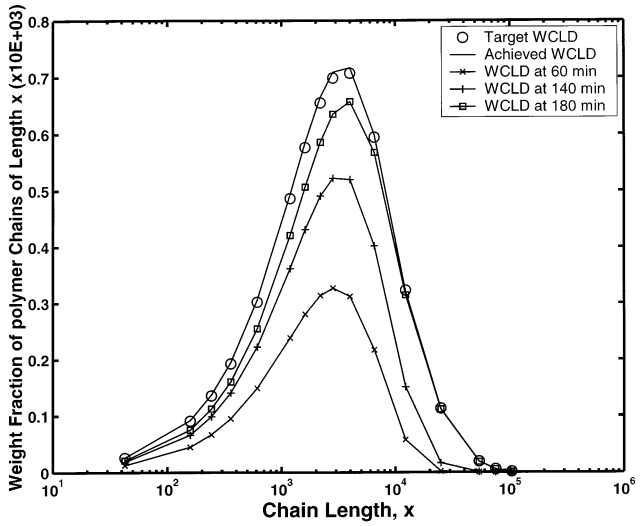

Figure 10. Time evolution of WCLD for grade B.

scenario. Notice that the total polymerization time increased from $t_f = 170$ min (e.g., nominal case) to $t_f = 242$ min to compensate for the effect of the time-varying termination rate constant on the product quality indicators. In Figure 9, the average molecular weights corresponding to the initial and updated temperature profiles for grade B are plotted with respect to the batch time. It should be pointed out that contrary to the calculated time optimal temperature profiles for grade A (see Figure 3), the time optimal temperature trajectories for grade B (e.g., a polymer grade with a low polydispersity index) exhibited a pike-shaped increase near the gel-effect region (see Figure 8). The increase in the polymerization temperature partially suppresses the large increase in the molecular weight due to the gel effect and lowers the value of the polydispersity index. Notice that the calculated time optimal temperature trajectories for grades A and B are consistent with the results of Thomas and Kiparissides.[13] Figure 10 shows the ability of the online optimizer to meet the specified WCLD at the final time. The present results clearly show that the proposed optimization/control framework has the ability to cope with parametric uncertainty in the termination rate constant while satisfying stringent and complex quality specifications.

Unknown Initial Conditions. Unknown amounts of reactive impurities in the monomer/solvent feed streams can influence the initiator efficiency and, thus, the polymerization rate and polymer molecular properties. Therefore, one needs first to estimate the effective initiator concentration in the reactor at time zero prior to the calculation of the time optimal temperature policy. In the present study, the estimation problem described by eqs 7 and 8 was solved to estimate the actual initiator concentration at time zero. The time horizon for the estimation of the initial initiator concentration extended from time zero until the instant of the last available measurement, implying that the length of the estimation horizon increased as the batch operation advanced.

In the simulated MMA batch reactor application, the initial initiator concentration was subjected to a 50% reduction from its nominal value because of the presence of reactive impurities. Monomer conversion and reactor/jacket temperatures comprised the available set of measurements. Monomer conversion and temperatures were corrupted by random noise with standard deviations of 0.2% and 0.2 K, respectively. The weight matrix $\mathbf{R}_{BE}$ in the estimator of eq 7 was assumed to be diagonal with elements equal to 5×10^{-4}, 50, and 50 for the three

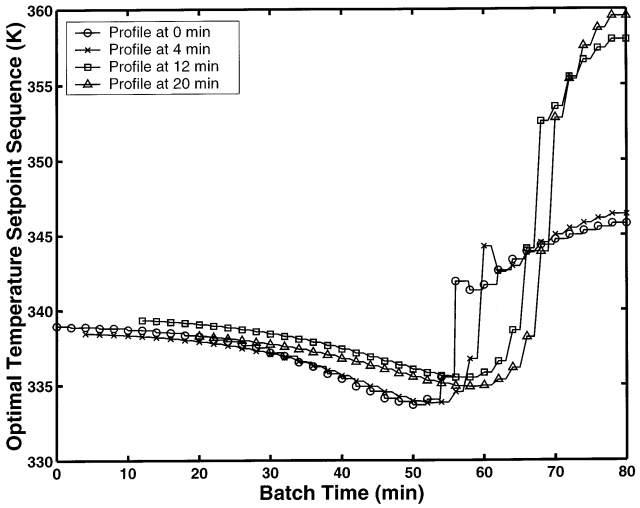

Figure 11. Updated time optimal temperature trajectories for the case of unknown initial initiator concentration.

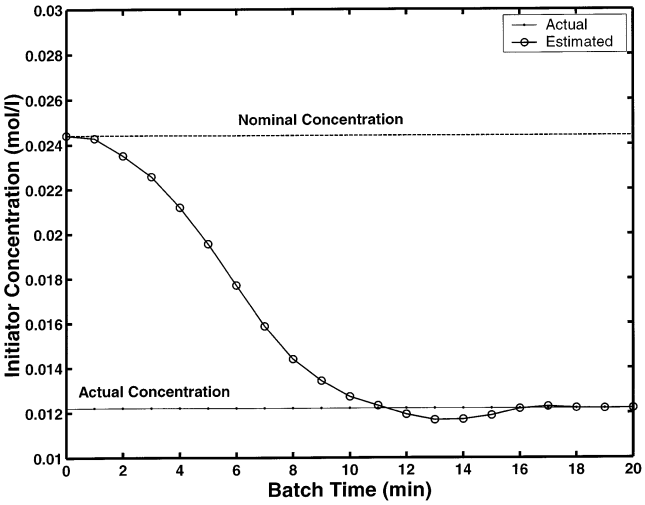

Figure 12. Nominal, actual, and estimated values of the initial initiator concentration.

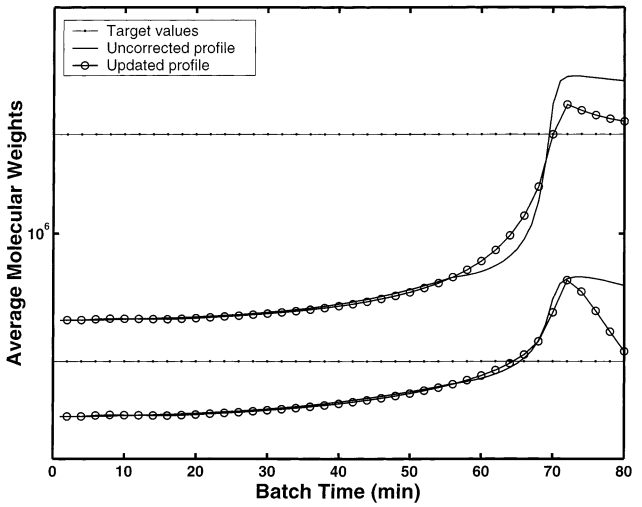

Figure 13. Uncorrected and updated number- and weight-average molecular weight profiles for the case of unknown initial initiator concentration.

measured quantities, respectively. On the other hand, in the present study the weight matrix $\mathbf{Q}_{BE}$ was set equal to zero for simplification. However, in a more general case a nonzero matrix $\mathbf{Q}_{BE}$ would account for the process−model mismatch. It should be also noted that the kinetic rate constant uncertainty at the early stages of the batch was assumed negligible. Matrix $\mathbf{P}_{0,BE}$ accounts for our confidence in the initial values of the unknown states. Because only the initial initiator concentration was assumed to be unknown, the single element of matrix $\mathbf{P}_{0,BE}$ was set equal to 5.0, a compromise between the convergence speed to the actual value and robustness to measurement noise. No target WCLD was specified for this simulated case, and the optimization was performed for fixed batch time.

The optimization-based batchwise estimator for the initial initiator concentration was solved every 1 min, while a new optimal control trajectory was computed every 4 min. In Figure 11, the updated sequence of temperature set-point changes are plotted at different time instances. It can be seen that the recalculated time optimal temperature trajectories maintain the characteristic shape of the initial profile (obtained at time 0 min). However, higher temperatures are, in general, required to achieve the specified product quality objectives as a result of the reduced initiator concentration due to the presence of reactive impurities. Notice that, after 20 min of batch operation, the estimated value of the initial initiator concentration converged to its true value (Figure 12) and, therefore, the optimization-based estimator was switched off. The observed small oscillations in the estimates of the initial initiator concentration were due to the noise in the process measurements and could be further smoothed by increasing the value of $\mathbf{P}_{0,BE}$. Finally, Figure 13 clearly depicts the significant improvement in the calculated values of the average molecular weights over the uncorrected ones.

Conclusions

An online estimation−optimization scheme has been developed to control the molecular weight averages as well as the WCLD in a free-radical batch polymerization reactor. The nonlinear estimator utilizes available online measurements on key process variables (e.g., monomer conversion and reactor and jacket temperatures) to provide reliable estimates of the state variables, time-varying model parameters, and unknown initial conditions. The online optimizer uses the updated values of the model parameters to calculate an optimal temperature sequence of set-point changes to ensure the satisfaction of product quality specifications. It was shown that the proposed estimation/control scheme can successfully compensate for the effect of a time-varying termination rate constant and the presence of unknown reactive impurities by proper adjustments in the online calculated time optimal temperature trajectory.

Appendix A. Batch Free-Radical Polymerization Model

The kinetic mechanism of a chemically initiated free-radical polymerization can be described in terms of the following elementary reactions:[25]

Initiation:

$$I \xrightarrow{k_d} 2R^\bullet$$

$$R^\bullet + M \xrightarrow{k_i} R_1$$

Propagation:

$$R_x + M \xrightarrow{k_p} R_{x+1} \qquad x = 1, 2, \ldots$$

Chain transfer to monomer:

$$R_x + M \xrightarrow{k_f} P_x + R_1 \qquad x = 1, 2, ...$$

Termination by disproportionation:

$$R_x + R_y \xrightarrow{k_{td}} P_x + P_y \qquad x, y = 1, 2, ...$$

Termination by combination:

$$R_x + R_y \xrightarrow{k_{tc}} P_{x+y} \qquad x, y = 1, 2, ...$$

The symbols I, R•, and M denote the initiator, the primary radicals, and the monomer, respectively. R_x and P_x are the corresponding "live" and "dead" polymer chains having a degree of polymerization x. Based on the above kinetic scheme, a set of ordinary differential equations can be derived to describe the conservation of the various molecular species in the batch reactor. In general, the states of the system are the volume of the reactive system, V, the monomer conversion, X, the initiator concentration, I, the leading moments of the "live" (λ_0, λ_1, and λ_2) and "dead" (μ_0, μ_1, and μ_2) NCLDs, and the reactor and jacket temperatures, T_R and T_J, respectively.

$$\frac{1}{V}\frac{dV}{dt} = \frac{\epsilon}{1+\epsilon X}\frac{dX}{dt} \tag{A1}$$

where ϵ is a volume contraction parameter defined as $\epsilon = (\rho_m - \rho_p)/\rho_p$.

$$\frac{dX}{dt} = (k_p + k_f)(\lambda_0 V)(1 - X)/V \tag{A2}$$

$$\frac{d(IV)}{dt} = -k_d IV \tag{A3}$$

$$\frac{d(\lambda_0 V)}{dt} = 2f_i k_d IV + (k_{tc} + k_{td})\lambda_0^2 V \tag{A4}$$

$$\frac{d(\lambda_1 V)}{dt} = 2f_i k_d IV + (k_f + k_p)M\lambda_0 V - [k_f M + (k_{tc} + k_{td})\lambda_0]\lambda_1 V \tag{A5}$$

$$\frac{d(\lambda_2 V)}{dt} = 2f_i k_d IV + (k_p + k_f)M\lambda_0 V + 2k_p M\lambda_1 V - [k_f M + (k_{tc} + k_{td})\lambda_0]\lambda_2 V \tag{A6}$$

$$\frac{d(\mu_0 V)}{dt} = \left[k_f M + \left(k_{td} + \frac{1}{2}k_{tc}\right)\lambda_0\right]\lambda_0 V \tag{A7}$$

$$\frac{d(\mu_1 V)}{dt} = [k_f M + (k_{tc} + k_{td})\lambda_0]\lambda_1 V \tag{A8}$$

$$\frac{d(\mu_2 V)}{dt} = [k_f M + (k_{tc} + k_{td})\lambda_0]\lambda_2 V + k_{tc}\lambda_1^2 V \tag{A9}$$

$$\frac{dT_R}{dt} = \left[\Delta H_R M_0 \frac{dX}{dt} - UA(T_R - T_J)/(V_{mix}\rho_{mix}Cp_{mix})\right] \tag{A10}$$

$$\frac{dT_J}{dt} = [UA(T_R - T_J) + F_{wj}\rho_w Cp_w(T_{J,in} - T_J)/(V_J\rho_w Cp_w)] \tag{A11}$$

The density and heat capacity of the reacting mixture can be calculated as follows:

$$\rho_{mix} = \left[\frac{X}{\rho_p} + \frac{(1-X)}{\rho_m}\right]^{-1} \tag{A12}$$

$$C_{\rho_{mix}} = C_{\rho_m}(1 - X) + C_{\rho_p}X \tag{A13}$$

To account for the effect of the diffusion-controlled phenomenon on the termination and propagation rate constants, the following gel- and glass-effect models were employed:[23]

$$k_t = k_{t0}g_t; \quad g_t = C/(C + \vartheta_t k_{t0}\lambda_0) \tag{A14}$$

$$k_p = k_{p0}g_p; \quad g_p = \frac{C}{C + \vartheta_p k_{p0}\lambda_0} \tag{A15}$$

$$\log C = (1 - \varphi_p)/[A + B(1 - \varphi_p)] \tag{A16}$$

where k_{t0} and k_{p0} are the termination and propagation rate constants at zero monomer conversion. φ_m and φ_p denote the monomer and polymer volume fractions expressed in terms of the monomer conversion and the volume contraction parameter, ϵ:

$$\varphi_m = (1 - X)/(1 + \epsilon X); \quad \varphi_p = 1 - \varphi_m \tag{A17}$$

From the known values of the "live" and "dead" moments, one can easily calculate the number- and weight-average molecular weights, M_n and M_w, as well as the polydispersity index, PD, of the polymer:

$$M_n = MW[(\mu_1 + \lambda_1)/(\mu_0 + \lambda_0)] \tag{A18}$$

$$M_w = MW[(\mu_2 + \lambda_2)/(\mu_1 + \lambda_1)] \tag{A19}$$

$$PD = M_w/M_n \tag{A20}$$

where MW is the molecular weight of the monomer.

Appendix B. MWD Calculations Using OCFE

Given the kinetic mechanism outlined in appendix A, the following balances for the "live" and "dead" polymer chains of chain length x ($x \in [2, S_f]$) are obtained:

$$\frac{dR_1}{dt} = k_i IM - k_p MR_1 - k_t R_1\sum_{y=1}^{\infty}R_y + k_f M\sum_{y=2}^{\infty}R_y \tag{B1}$$

$$\frac{dR_x}{dt} = k_p MR_{x-1} - k_p MR_x + k_f MR_x - k_t R_x\sum_{y=1}^{\infty}R_y \tag{B2}$$

$$\frac{dP_x}{dt} = k_f MR_x + k_{td}R_x\sum_{y=1}^{\infty}R_y + k_{tc}\sum_{y=1}^{x-1}(R_y R_x - R_y) \tag{B3}$$

Assuming that the pseudo-steady-state approximation for "live" polymer chains of length x holds true, the following relationships can be derived for the "live" polymer chains:

$$R_1 = (1 - r)\lambda_0 \tag{B4}$$

$$R_x = r^{x-1}(1 - r)\lambda_0 \tag{B5}$$

where r is the propagation rate probability defined as

$$r = k_p M/(k_p M + k_f M + k_t \lambda_0) \qquad \text{(B6)}$$

Following the developments of Seferlis et al.,[21] the concentration of the "dead" polymer chains is approximated in terms of Lagrange interpolation polynomials:

$$\tilde{P}(s) = \sum_{i=1}^{n} W_{i,j}^{p}(s)\, \tilde{P}(s_{i,j}) \qquad \zeta_{j-1} \le s \le \zeta_j; \quad j = 1, ..., N_x \qquad \text{(B7)}$$

The tilde denotes approximation variables. $W_{i,j}^{p}(s)$ represents the Lagrange interpolation polynomial of order n:

$$W_{i,j}^{p}(s) = \prod_{\substack{k=1 \\ k \neq i}}^{n} \frac{s - s_{k,j}}{s_{i,j} - s_{k,j}}; \qquad \zeta_{j-1} \le s \le \zeta_j; \quad i = 1, ..., n; \quad j = 1, ..., N_x \qquad \text{(B8)}$$

By substitution of eq B5 into eq B3, the following expression for the concentration of the "dead" polymer chains at the collocation points is obtained:

$$\frac{dP(s_{i,j})}{dt} = (k_f M + k_{td}\lambda_0)(1-\rho)\rho^{s_{i,j}-1} + \left(\frac{k_{tc}}{2}\lambda_0^{\,2}\right)(1-\rho)^2\rho^{s_{i,j}-2}(s_{i,j}-1) \qquad \text{(B9)}$$

The collocation points are chosen as the roots of the discrete Hahn family of orthogonal polynomials. The selection of the Hahn orthogonal polynomials is mainly supported from the structural asymptotic behavior of the resulting OCFE formulation. At the limiting case, where the total number of collocation points equals the achieved degree of polymerization, the OCFE formulation matches exactly the full-order model (see eqs B2 and B3).

The residual equations are then integrated in time to calculate the evolution of the concentrations of the "dead" polymer chains at the selected collocation points. Based on the calculated values, $\tilde{P}(s_{i,j})$, the WCLD can easily be reconstructed using the following equation:

$$\mathrm{WCLD}_{x_{i,j}} = s_{i,j}\tilde{P}(s_{i,j})/\sum_{s=2}^{S_f} s\tilde{P}(s) \qquad \text{(B10)}$$

Notice that the denominator in eq B10 is equal to the first moment of the WCLD of the "dead" polymer chains, μ_1. In general, the accuracy of the OCFE approximation will depend on the total number of collocation points ($N_x \times n$), the element partition ($\zeta_0 = 1, \zeta_1, \zeta_2, ..., \zeta_{N_x-1}, \zeta_{N_x} = S_f$), and the size of the chain-length domain, S_f.

Notation

C = state variable constraint matrix
C_p = heat capacity, kJ/(kg K)
d = vector of model parameters and process disturbances
f = vector of process model equality constraints
f_i = initiator efficiency
g = vector of process model inequality constraints
h = vector of process model constraints (measured variables)
I = initiator concentration, kmol/m^3
K = EKF gain matrix
k_d = initiation rate constant, 1/min
k_f = chain transfer to monomer rate constant, m^3/(kmol min)
k_p = propagation rate constant, m^3/(kmol min)
k_t = termination rate constant, m^3/(kmol min)
k_{tc} = termination by combination rate constant, m^3/(kmol min)
k_{td} = termination by disproportionation rate constant, m^3/(kmol min)
M = monomer concentration, kmol/m^3
M_n = number-average molecular weight, kg/kmol
M_w = weight-average molecular weight, kg/kmol
MW = molecular weight, kg/kmol
N_e = number of temporal finite elements
N_x = number of chain-length finite elements
P = EKF and optimization-based batchwise estimator tuning matrix
P_x = concentration of "dead" polymer chains of length x, kmol/m^3
PD = polydispersity index
Q = EKF and optimization-based batchwise estimator tuning matrix
R = EKF and optimization-based batchwise estimator tuning matrix
R_x = concentration of "live" polymer chains of length x, kmol/m^3
r = propagation rate probability
S_f = collocation chain-length domain
t = time, min
T_J = reactor jacket temperature, K
T_R = reactor temperature, K
U = heat-transfer coefficient, kJ/(m^2 K min)
v = vector of measurement noise
V = reactive mixture volume, m^3
w = vector of process noise
x = vector of state variables
x = chain length
X = monomer conversion
y = vector of measured (output) variables

Greek Symbols

ΔH_R = heat of reaction, kJ/mol
ϵ = volume expansion factor
ζ = chain-length element breakpoint
λ = moment of the number chain-length distributions of the "live" polymer chains
μ = moment of the number chain-length distributions of the "dead" polymer chains
ρ = density, kg/m^3
τ = temporal element breakpoint
φ = volume fraction

Literature Cited

(1) Ponnuswamy, S. R.; Shah, S. L.; Kiparissides, C. Computer optimal control of batch polymerization reactors. *Ind. Eng. Chem. Res.* **1987**, *26*, 2229.

(2) Ruppen, D.; Benthack, C.; Bonvin, D. Optimization of batch reactor operating under parametric uncertainty—computational aspects. *J. Process Control* **1995**, *5*, 235.

(3) Ruppen, D.; Bonvin, D.; Rippin, D. W. T. Implementation of adaptive optimal operation for a semi-batch reaction system. *Comput. Chem. Eng.* **1997**, *22*, 185.

(4) Levien, K. L. Maximizing the product distribution in batch reactors: Reactions in parallel. *Chem. Eng. Sci.* **1992**, *47*, 1751.

(5) Loeblein, C.; Perkins, J. D. Economic analysis of different structures of on-line process optimization systems. *Comput. Chem. Eng.* **1996**, *20*, S551.

(6) Crowley, T. J.; Choi, K. Y. Discrete optimal control of molecular weight distribution in a batch free-radical polymerization process. *Ind. Eng. Chem. Res.* **1997**, *36*, 3676.

(7) Crowley, T. J.; Choi, K. Y. Experimental studies on optimal molecular weight distribution control in batch free-radical polymerization process. *Chem. Eng. Sci.* **1998**, *53*, 2769.

(8) De Valliere, P.; Bonvin, D. Application of estimation techniques to batch reactors. III. Modelling refinements which improve the quality of state and parameter estimation. *Comput. Chem. Eng.* **1990**, *14*, 799.

(9) Gagnon, L.; MacGregor, J. F. State Estimation for continuous emulsion polymerization. *Can. J. Chem. Eng.* **1991**, *69*, 648.

(10) Kozub, D. J.; MacGregor, J. F. State estimation for semi-batch polymerization reactors. *Chem. Eng. Sci.* **1992**, *47*, 1047.

(11) Muske, K. R.; Rawlings, J. B.; Lee, J. H. Receding horizon recursive state estimation. In *Methods of Model Based Process Control*; Berber, R., Ed.; Kluwer Academic Publishers: Dordrecht, The Netherlands, 1995.

(12) Bryson, A. E.; Ho, Y. C. *Applied Optimal Control*; John Wiley & Sons: New York, 1975.

(13) Thomas, I. M.; Kiparissides, C. Computation of the near-optimal policies for a batch polymerization reactor. *Can. J. Chem. Eng.* **1984**, *62*, 284.

(14) Renfro, J. G. Computational Studies in the Optimization of Systems described by Differential-Algebraic Equations. Ph.D. Dissertation, University of Houston, Houston, TX, 1986.

(15) Cuthrell, J. E.; Biegler, L. T. On the optimization of differential-algebraic process systems. *AIChE J.* **1987**, *33*, 1257.

(16) Tjoa, L.-B.; Biegler, L. T. Simultaneous solution and optimization strategies for parameter estimation of differential-algebraic equation systems. *Ind. Eng. Chem. Res.* **1991**, *30*, 376.

(17) Vassiliadis, V. S.; Sargent, R. W. H.; Pantelides, C. C. Solution of a class of multistage dynamic optimization problems. 2. Problems with path constraints. *Ind. Eng. Chem. Res.* **1994**, *33*, 2123.

(18) Russel, R. D.; Christiansen, J. Adaptive mesh selection strategies for solving boundary value problems. *SIAM J. Numer. Anal.* **1978**, *15*, 59.

(19) Seferlis, P.; Hrymak, A. N. Adaptive collocation on finite elements models for the optimization of multi-stage distillation units. *Chem. Eng. Sci.* **1994**, *49*, 1369.

(20) Koster, L. G.; Gazi, E.; Seider, W. D. Finite elements for near-singular systems: application to bacterial chemotaxis. *Comput. Chem. Eng.* **1993**, *17*, 485.

(21) Seferlis, P.; Keramopoulos, A.; Kiparissides, C. A novel method for the prediction of the molecular weight distribution in free radical polymerizations using orthogonal collocation on finite elements. Submitted for publication in *Chem. Eng. Sci.*

(22) Murtagh, B. A.; Saunders, M. A. *MINOS 5.1 User's Guide*; Technical Report SOL 83-20R; Stanford University: Stanford, CA, 1990.

(23) Chiu, W. Y.; Carratt, G. M.; Soong, D. S. A computer model for the gel effect in free-radical polymerization. *Macromolecules* **1983**, *16*, 348.

(24) Louie, B. M.; Soong, D. S. Optimization of batch polymerization Processes—Narrowing the MWD. I. Model simulation. *J. Appl. Polym. Sci.* **1985**, *30*, 3707.

(25) Achilias, D. S.; Kiparissides, C. Development of a general mathematical framework for modelling diffusion-controlled free-radical polymerization reactions. *Macromolecules* **1992**, *25*, 3739.

Received for review April 16, 2001
Revised manuscript received July 23, 2002
Accepted September 13, 2002

IE0103409